Dissociations in Coherence Sensitivity Reveal Atypical Development of Cortical Visual Processing in Congenital Achromatopsia

Eliza Burton,[1] John Wattam-Bell,*[,2] Gary S. Rubin,[1] Jonathan Aboshiha,[1,3] Michel Michaelides,[1,3] Janette Atkinson,[2,4] Oliver Braddick,[4] and Marko Nardini[1,5]

[1]Institute of Ophthalmology, University College London, London, United Kingdom
[2]Division of Psychology and Language Sciences, University College London, London, United Kingdom
[3]Moorfields Eye Hospital, London, United Kingdom
[4]Experimental Psychology, University of Oxford, Oxford, United Kingdom
[5]Department of Psychology, Durham University, Durham, United Kingdom

Correspondence: Eliza Burton, UCL Institute of Ophthalmology, 11-43 Bath Street, London EC1V 9EL, UK; eliza.burton@ucl.ac.uk.
Marko Nardini, Psychology Department, Durham University, Science Laboratories, South Road, Durham DH1 3LE, UK; marko.nardini@durham.ac.uk.

*Deceased December 30, 2013

Submitted: October 14, 2015
Accepted: February 26, 2016

Citation: Burton E, Wattam-Bell J, Rubin GS, et al. Dissociations in coherence sensitivity reveal atypical development of cortical visual processing in congenital achromatopsia. *Invest Ophthalmol Vis Sci*. 2016;57:2251–2259. DOI:10.1167/iovs.15-18414

Purpose. While basic visual functions have been described in subjects with congenital achromatopsia (ACHM), little is known about their mid- or high-level cortical visual processing. We compared midlevel cortical visual processing in ACHM subjects ($n = 11$) and controls ($n = 20$).

Methods. Abilities to detect global form, global motion, and biological motion embedded in noise were tested across a range of light levels, including scotopic, in which both ACHM subjects and controls must rely on rods. Contrast sensitivity functions (CSFs) were also measured.

Results. Achromatopsia subjects showed differential impairments across tests. In scotopic conditions, global form was most impaired, while biological motion was normal. In a subset of three ACHM subjects with normal scotopic CSFs, two of the three showed global form perception worse than controls; all showed global motion comparable to controls; and strikingly, two of the three showed biological motion perception superior to controls.

Conclusions. The cone signal appears to play a crucial role in the development of perception of global form, as in ACHM this is impaired even in scotopic conditions, in which controls also have to rely on rods, and even in ACHM subjects with no scotopic spatial vision loss. In contrast, the rod signal appears sufficient for the development of normal (or even superior) extrastriate biological motion perception. These results suggest that ACHM leads to atypical development of cortical vision, highlighting the need to better understand the potential for further reorganization of cortical visual processing following new therapies aimed at restoring cone function.

Keywords: motion perception, form perception, psychophysics, biological motion, rod vision

Achromatopsia (ACHM), also known as rod monochromacy, is a stationary cone dysfunction syndrome, affecting ~1 in 30,000 people.[1,2] The main symptoms are reduced visual acuity, photophobia, and an absence of color vision from birth/early infancy. Individuals with ACHM prefer mesopic conditions and have normal night vision. Transmission is autosomal recessive, and six genes have been identified: *GNAT2*, *PDE6C*, *PDE6H*, *ATF6*, *CNGA3*, and *CNGB3*, which together account for approximately 70% to 80% of all cases.[1,3] Of these, ~70% of cases are caused by mutations in either *CNGA3* or *CNGB3*.[4] While classified as a stationary disorder, there is evidence of changes to the retina over time,[5–7] although the extent to which this may impact functional vision is unclear.

Previous research into visual function in ACHM has focused on early-level visual functions such as acuity and contrast sensitivity.[2,8–15] For example, visual acuity in ACHM subjects with *CNGA3* and *CNGB3* mutations has been reported in the range of 20/100 to 20/600.[16] Spatial and temporal acuity as well as contrast sensitivity has been reported as impaired in photopic conditions in ACHM. Under scotopic conditions, these functions have, in some cases, been reported as comparable to controls, suggesting typical rod-mediated basic vision,[9–11] although atypical dark adaptation curves have also been observed.[17–19]

In the present study we examined for the first time midlevel cortical visual functions in congenital ACHM, specifically, global form, global motion, and biological motion perception. These have all been studied extensively in both typically developing[20–23] and atypical populations,[24–29] and depend on extrastriate cortical visual areas known from animal models and human neuroimaging.[25,30–36]

To examine the effects of ACHM on global form and motion processing, it is necessary to consider whether low-level impairments of contrast sensitivity and the restriction to rod function play a role in any reduction of sensitivity. We have attempted to simulate these effects with normal observers by testing global form and motion sensitivity with a diffusing screen that acts as a low-pass filter for spatial frequencies[37] and

Table. Demographic and Clinical Details for the 11 Achromatopsia Subjects With Established Genotypes

				Visual Acuity, logMAR			Contrast Sensitivity, LogCS		Fixation Stability, %*		
Subject	Age	Sex	Genotype	Right Eye	Left Eye	Both Eyes	Right Eye	Left Eye	Both Eyes	Right Eye	Left Eye
S1	19.6	F	*CNGA3*	0.78	0.78	0.78	NA	NA	NA	NA	NA
S2	20.6	M	*CNGB3*	0.88	0.86	0.82	1.35	1.35	1.5	100	87
S3	21.2	F	*CNGA3*	0.8	0.8	0.76	0.75	0.65	0.9	100	100
S4	25.3	M	*CNGB3*	0.72	0.8	0.64	1.75	1.55	1.85	100	96
S5	26.8	M	*CNGB3*	0.84	0.92	0.82	1.5	1.2	1.4	99	99
S6	28.5	M	*CNGB3*	1	1.2	1	1.05	1.15	1.35	30	27
S7	31.5	M	*CNGB3*	0.86	0.84	0.84	1.35	1.35	1.4	85	99
S8	34	F	*CNGA3*	0.9	0.84	0.82	1.5	1.5	1.65	91	79
S9	35.8	F	*CNGB3*	0.88	1.1	0.88	1.05	1.1	1.2	NA	NA
S10	42.3	F	*CNGA3*	1	1	1	NA	NA	NA	NA	NA
S11	50	M	*CNGB3*	0.92	1	0.86	1.35	1.15	1.35	100	92

* Fixation was recorded with a Nidek MP1 microperimeter. Participants were required to fixate a cross subtending 2°. The number given is the percentage of time spent fixating the central 4° surrounding the fixation target over a 30-second period.

by testing under scotopic levels of illumination.[38] Both methods have been used and reported in previous studies: blur[39–41] and scotopic illumination.[42–45] Our recent study of global form, motion, and biological motion processing[38] with healthy controls (the same data provide a comparison for ACHM subjects in this paper) found greater impairments in global form perception under low light relative to global motion and biological motion. This implies that rod vision is relatively more efficient for processing global motion than global form. These results imply that, compared with controls at photopic light levels, ACHM subjects may show impairments in form relative to motion and biological motion perception due to a reliance on rods for vision in the latter cases. A crucial comparison, however, is between controls and ACHM subjects at scotopic light levels, at which both groups must rely on rods. In scotopic conditions, ACHM subjects may differ from controls if they have atypical rod functioning and/or have undergone atypical visual development due to experiencing atypical (rod-only) visual input from birth. This comparison is the focus of the present paper.

Methods

Subjects

Eleven subjects (mean age, 28.6; standard deviation, 7.4 years; range, 19.6–50.0 years; 6 males/5 females) with a diagnosis of ACHM completed the study within the Faculty of Brain Sciences, Division of Psychology and Language Sciences, University College London. Information sheets were provided and informed consent was obtained before testing commenced. All research procedures were carried out in accordance with the guidelines of the Declaration of Helsinki. Results were compared with baseline data collected from 20 normally sighted control subjects (mean age, 25.2; standard deviation, 4.6 years; range, 18.9–38.0 years; 11 males/9 females), which have been reported in detail elsewhere.[38]

Achromatopsia subjects were recruited through referrals from their clinician (JA, MM) at Moorfields Eye Hospital. All subjects had a diagnosis of ACHM based on both clinical symptoms and genotyping. Details of genotype and visual acuity for each subject can be found in the Table. Details of contrast sensitivity and of fixation stability, recorded using a Nidek MP-1 microperimeter (Nidek Technologies, Padova, Italy), are also given where these test results were available. Acuity and contrast sensitivity tests were carried out using standard protocols and lighting conditions (85 cd/m^2). Microperimetry was carried out on a research basis, and results have been published elsewhere.[5]

Stimulus Generation and Task Design

Stimuli were generated in MATLAB 2012 (MathWorks, Natick, MA, USA) using the Psychophysics Toolbox extensions.[46–48] Stimuli were viewed on a Mitsubishi (Tokyo, Japan) Diamond Pro SB2070 22-inch cathode ray tube (60-Hz refresh rate) at a distance of 60 cm with a display area of 37° × 28°. This display distance reduced the need to accommodate close up, therefore reducing the impact of any hyperopic refractive error. Individuals with prescription lenses wore these during the study.

Testing took approximately 1 hour per subject, with additional time required for the dark adaptation. Each task (form, motion, biological motion) was repeated three times in each light condition. The contrast sensitivity task was completed in one run in each light condition. The order of the four tasks was randomized for each light condition; however, the three runs of each task were always carried out in succession so that a subject completed 90 trials of form, motion, or biological motion consecutively.

Global Form and Motion Stimuli

Example form and motion stimuli are shown in Figure 1. These stimuli have been used and described in previous studies.[37,38,49,50] The stimuli were designed to be matched in terms of the regions of the visual field over which form or motion needs to be integrated.

The task was to judge which side of the display, left or right, contained the global stimulus. Coherence of stimuli (proportion of coherent, as compared with random, elements) was varied to estimate coherence thresholds. Both the form and motion stimuli were constructed from 2000 white dots (each 6 pixels in diameter, 0.29° visual angle) against a black background. For the motion stimulus, dots were plotted in successive frames along an arc trajectory, moving at 8.6°/s, with a lifetime of 133 ms. For the form stimulus, dots were plotted simultaneously to create short line segments. Motion trajectories and line segments could be up to eight dots in length. For the motion stimulus, within each frame 1/8th of the number of dots were restarted in a random location, creating a range of trajectory lengths. In the form stimulus in which short line segments were based on these trajectories, this created lines ranging from one to eight dots in length, averaging 1.3°.

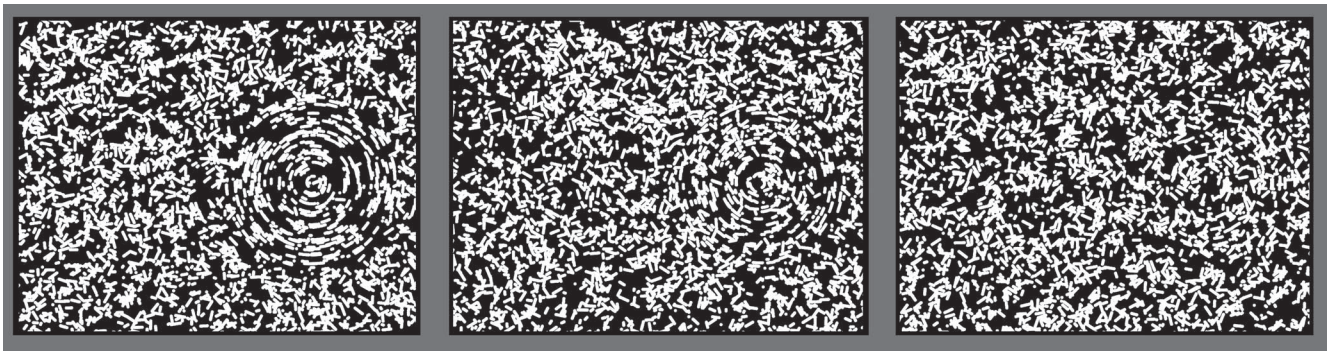

FIGURE 1. Example stimuli for the form and motion task. Stimuli from *left* to *right* show 91%, 60%, and 24% coherence (with the global pattern always on the *right*). Form stimuli are shown here, but also demonstrate the motion task in which each line segment represents the motion trajectory of a single dot.

Motion dots and form short line segments were randomly distributed across the display. Coherent elements were plotted around a common center of curvature, creating a circular structure subtending 16°. Incoherent elements were randomly oriented.

On each trial, global form or motion was plotted, at random, on one side of the display (centered 10° from the display center). The opposite side always contained incoherent stimuli. Subjects were asked to fixate a central point while stimuli were displayed for 1 second. Subjects then had as long as they needed following this to indicate (with a button press) via two-alternative forced choice (2AFC) on which side they had seen the coherent pattern. The level of coherence was varied from trial to trial according to the PSI adaptive method.[51] Subjects completed 90 trials per light level of the form and motion tests, each made up of three runs of 30 trials. The 75% coherence threshold was calculated for each run, and estimated thresholds were averaged across three runs.

Biological Motion

The biological motion stimulus consisted of a point-light figure walking on the spot (see Fig. 2). The angle of the walker around the vertical was randomly varied from trial to trial to reduce habituation and predictability of the stimulus. The stimulus was generated using Cutting's algorithm,[52] creating figures made up of 14 white dots each with a visual angle of 0.27° and subtending 15.2° × 5.7° in total. Dots moved at an average speed of 5.8°/s.

As with the form and motion test, the biological motion test employed a 2AFC design. Biological motion was presented on one side of the display while a scrambled version was presented on the opposite side. Scrambled figures had the starting positions of dots and phase of joint angles randomized. Subjects were asked to indicate which side of the display contained the unscrambled biological motion. Figures were embedded within random noise dots. Noise dots moved at the same average speed as the biological motion dots (5.8°/s) and were drawn at random from the individual motion trajectories of biological motion dots. The proportion of signal to noise dots varied from trial to trial based on the PSI adaptive method. As with the form and motion tests, subjects completed 90 trials per light condition (three runs of 30 trials) and the 75% threshold was estimated based on the average threshold across these three runs.

Contrast Sensitivity Test

In addition to form, motion, and biological motion, contrast sensitivity functions (CSFs) were also measured. These provided a measure of early-level visual processing. Contrast sensitivity functions were measured for all controls and 9 of the 11 ACHM subjects (2 subjects were unable to attend for this second CSF testing session). Contrast sensitivity functions were recorded using the qCSF method,[53] which is based on a Bayesian adaptive procedure and fits the CSF by estimating four parameters of the curve.

The qCSF test used a 2AFC procedure in which subjects were asked to indicate the location of a Gabor patch of variable carrier spatial frequency, set within a 6° standard deviation Gaussian envelope matched in average luminance to the background. The test displayed spatial frequencies within the range of 0.56 to 13.75 cyc/deg and contrasts within the range of 0.5% to 97% (Michelson contrast). The Gabor was always placed at random, 10° to the left or right of central fixation. Subjects completed 100 trials per light level.

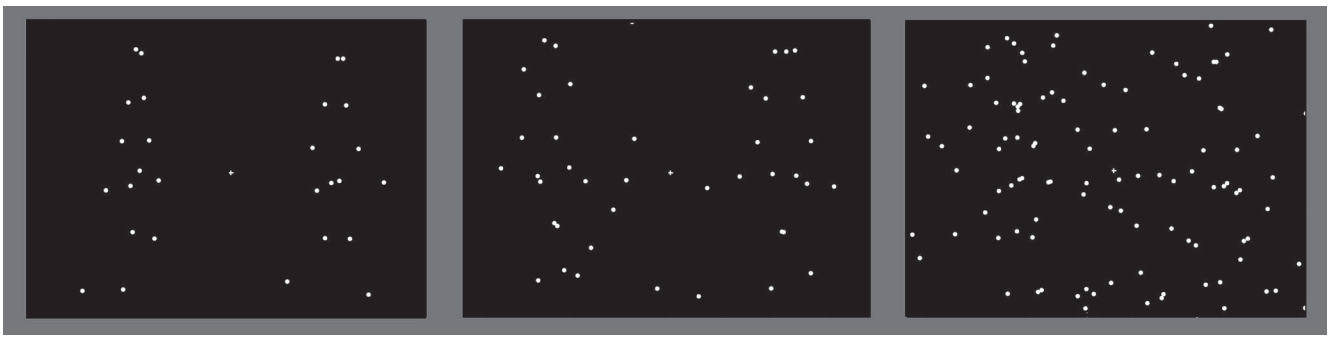

FIGURE 2. Example of the biological motion stimulus display at 93%, 50%, and 15% signal-to-noise ratio. Biological motion is present on the *right* of these stimuli, scrambled motion on the *left*.

Investigative Ophthalmology & Visual Science

Light Levels

Subjects completed all the tests at four light levels. These were defined as photopic (8.7 cd/m^2), high mesopic (0.8 cd/m^2), low mesopic (2.7×10^{-2} cd/m^2), and scotopic (8.7×10^{-4} cd/m^2). For the global form, motion, and biological motion tests, the reported luminances are those of the dots or lines, which were plotted against a black background. Contrast for these tests was kept constant at each light level at 3.24 Log Weber Contrast (LogWC). In the case of the contrast sensitivity test the luminance refers to the background luminance. The different light levels were obtained using neutral density filters (Sabre International Ltd., Reading, UK), which were placed over the display monitor. No other light sources were present in the room, which was also shielded from stray external light.

The order of light levels was counterbalanced so that half of the subjects completed the high mesopic and photopic conditions first while half completed the scotopic and low mesopic first. All subjects were dark adapted before the tests. Thirty minutes of dark adaptation took place before the scotopic/low mesopic tests, and 10 minutes of adaptation took place before the high mesopic/photopic conditions. Adaptation was achieved using blackout goggles (Mindfold, Inc., Durango, CO, USA).

Analyses

Results from all four light level conditions are given in Supplementary Figure S1, but to streamline our presentation and analyses we focus here on the photopic and scotopic conditions. The scotopic condition is crucial as it is the one in which controls and ACHM subjects are theoretically matched in relying only on rods, while the photopic condition is the one that is optimal for controls.

We used 2-way repeated-measures ANOVAs to compare (log transformed) discrimination thresholds of ACHM subjects and controls by light level on each test. We then examined CSF results and carried out an additional analysis on the subset of ACHM subjects who showed normal scotopic CSFs. We used 1-sample *t*-tests corrected for multiple comparisons to compare scotopic global form, motion, and biological motion sensitivity in these individual subjects with the group of controls.

Results

Global Form, Global Motion, and Biological Motion

The Shapiro-Wilk test of normality (Supplementary Table S1) was used to check whether coherence thresholds departed from normal distributions in each test and subject group. These revealed that many results were not normally distributed. Therefore, all coherence thresholds were log transformed for further analysis. Following log transformation, none of the data departed from a normal distribution as shown in Supplementary Table S1. An example of the shift to a normal distribution is given in Supplementary Figure S2, which shows the distribution of one set of data before and after log transformation. Group coherence thresholds, prior to log transformation, can be seen in Supplementary Figure S1.

Figure 3 shows log behavioral thresholds for ACHM subjects and controls in photopic and scotopic conditions. To test for differences between groups and light levels in each test, we used 2-way repeated-measures ANOVAs with the between-subjects factor group (control or ACHM) and the within-subjects factor light level (photopic or scotopic). Overall, ACHM subjects were significantly worse than controls (main effect of group) on the global form ($F[1,29] = 21.867$, $P < 0.001$) and global motion ($F[1,29] = 12.878$, $P = 0.001$) tests but not on the biological motion test ($F[1,29] = 2.317$, $P = 0.139$). There was a significant main effect of light level on all three tests (form: $F(1,29) = 92.103$, $P < 0.001$; motion: $F[1,29] = 29.512$, $P < 0.001$; biological motion: $F[1,29] = 54.971$, $P < 0.001$), corresponding to worse performance under scotopic conditions. There was also a significant group × light level interaction for all three tests (form: $F[1,29] = 4.666$, $P = 0.039$; motion: $F[1,29] = 6.417$, $P = 0.017$; biological motion: $F[1,29] = 4.657$, $P = 0.039$). This suggests that light affected sensitivity differently in the two groups. This can be seen in Figure 3, with ACHM subjects' thresholds increasing less markedly in scotopic conditions than those of controls. The main conclusions of this analysis are also supported by a direct comparison between the three tests through conversion to *z* scores (see Supplementary Fig. S3).

Contrast Sensitivity Functions

Figure 4 shows measured photopic and scotopic CSFs for each ACHM subject. Full CSF data from all four light levels are shown in Supplementary Figure S4. Two of the ACHM subjects were unable to attend follow-up appointments to have their CSFs measured, so results are given for 9 of 11 of the ACHM subjects. The CSF curves represent log contrast sensitivity across a range of spatial frequencies. Shaded regions represent the 95% confidence intervals (CIs) of control data for each light condition, while solid lines represent the individual ACHM subjects' results in photopic (blue) and scotopic (red) conditions. Subjects' CSFs falling within the 95% CI are therefore comparable to those of controls. This was expected only under scotopic light levels. Three ACHM subjects (S5, S7, S10; Fig. 4, marked with † symbol) had scotopic CSFs (red curves in Fig. 4) comparable to those of controls. Two of the nine ACHM subjects had severe difficulties with the task, with recordable responses only in the high mesopic condition and no recordable responses in photopic or scotopic conditions (S1 and S11; Fig. 4, marked with ‡ symbol). For these ACHM subjects the CSF task was particularly difficult relative to the midlevel tests.

Form, Motion, and Biological Motion Perception in ACHM Subjects With Normal Scotopic CSFs

As Figure 4 shows, three of the nine ACHM subjects whose CSFs were measured had scotopic CSFs (red curves) at least within the control range (S5, S7, and S10; S10 had scotopic sensitivity better than the 95% control range at low spatial frequencies). These results show that there was considerable variability in spatial vision in the ACHM group. Achromatopsia subjects with scotopic CSFs comparable to those of controls (S5, S7, and S10) had their scotopic form, motion, and biological results further examined.

Figure 5 shows control group data in the scotopic condition, plotted alongside the individual data from ACHM subjects. The three ACHM subjects with scotopic CSFs comparable to those of controls (S5, S7, and S10, marked as O's in Fig. 5) had elevated scotopic form thresholds compared to controls. However, their motion and biological motion thresholds were comparable to or better than the ACHM group average (see Fig. 5). Their motion thresholds were within or just outside the control 95% CI, and their biological motion perception was notably good, with two of the three ACHM subjects (S7 and S10) showing biological motion thresholds better than the control 95% CI (Fig. 5).

Departures from the control 95% CI in Figure 5 are informative, but to test stringently for significant differences against controls in this subset of ACHM subjects, we adjusted for the three multiple comparisons (i.e., three individuals

Investigative Ophthalmology & Visual Science

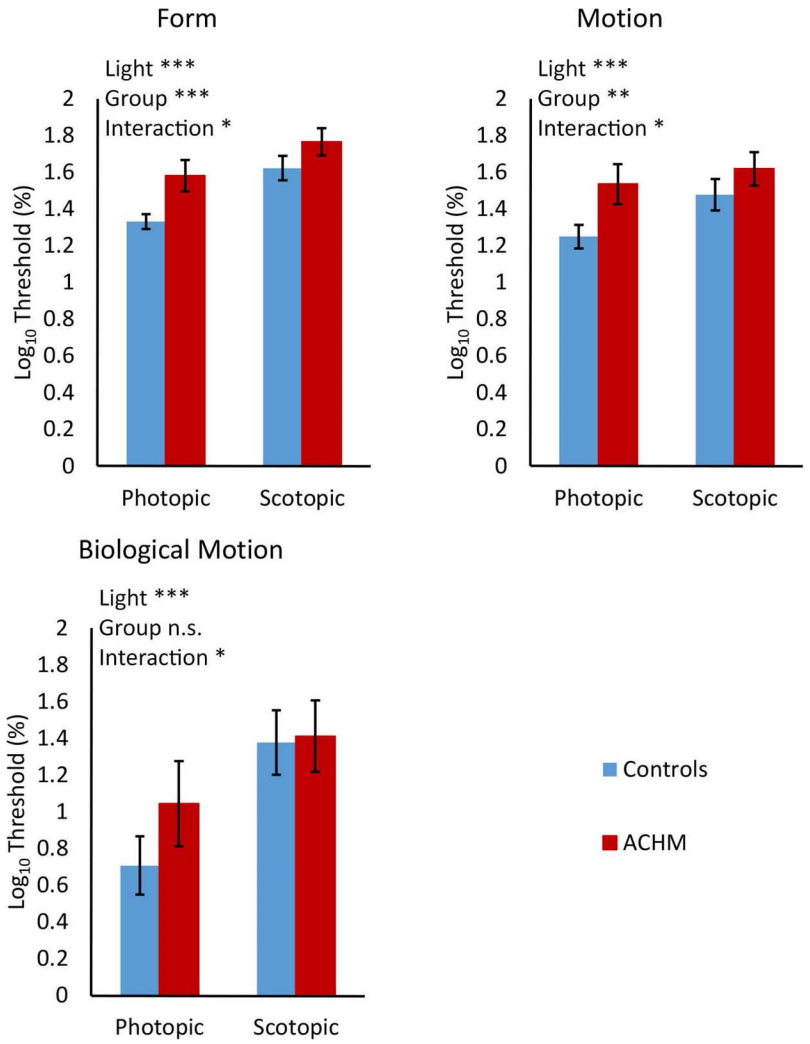

FIGURE 3. Achromatopsia and control mean $\log_{10}$ coherence thresholds for form, motion, and biological motion tasks under two light levels. *Error bars* represent 95% confidence intervals. ANOVA results are summarized at the *top of each graph*: for light (photopic/scotopic), for group (control/ACHM), and for the light × group interaction, $^{***}P < 0.001$, $^{**}P < 0.01$, $^{*}P < 0.05$; n.s. nonsignificant.

considered in Fig. 5) in each test. We asked whether each subject's log threshold differed from the control group mean using a 2-tailed 1-sample *t*-test, with a significance threshold calculated using the Šidák correction to give a family-wise type I error rate of 0.05 (the corrected *P* value is 0.0170). Significant results from these tests are indicated in Figure 5 (marked with * symbol). As Figure 5 shows, two of three ACHM subjects demonstrated biological motion perception superior to that of controls in scotopic conditions (the remaining subject was comparable to controls), and three of three demonstrated global motion perception comparable to that of controls. However, even in these ACHM subjects with normal scotopic CSFs, two of three showed impaired global form perception.

Neither individual differences in CSFs (Fig. 4) nor patterns of performance on the main tasks in those ACHM subjects with normal scotopic CSFs (Fig. 5) are well accounted for by differences in age or genotype (see Table). These three subjects had ages (31.5, 26.8, and 42.3 years) within the middle of the overall range for the ACHM group (19.6–50.0 years) and had both *CNGB3* ($n = 2$) and *CNGA3* ($n = 1$) mutations. The ACHM subjects with superior biological motion perception (S7 and S10) were the older two, one with each of *CNGA3* and *CNGB3*. In those with minimal CSF responses (S1, S11) there is also no consistency in age or genotype, suggesting that these factors do not explain their results.

DISCUSSION

The study aimed to understand the impact of ACHM on midlevel visual perception. We were particularly interested in whether an absence of cones leads to differences in cortical visual processing that are not explained simply by changes in low-level visual perception. Such differences compared with controls could be due to visual development with atypical input.

Results showed that ACHM subjects had differential impairments in midlevel vision across different tests. Analyses of variance of log thresholds found most evidence for impairments of global form and motion, rather than biological motion. Tests in scotopic conditions in which ACHM subjects and controls are both dependent on their rods for vision revealed impairments in global form and motion perception but normal biological motion perception.

These results suggest that a congenital absence of cones allows for normal or near-normal development of some kinds of (scotopic) midlevel visual processing, including biological

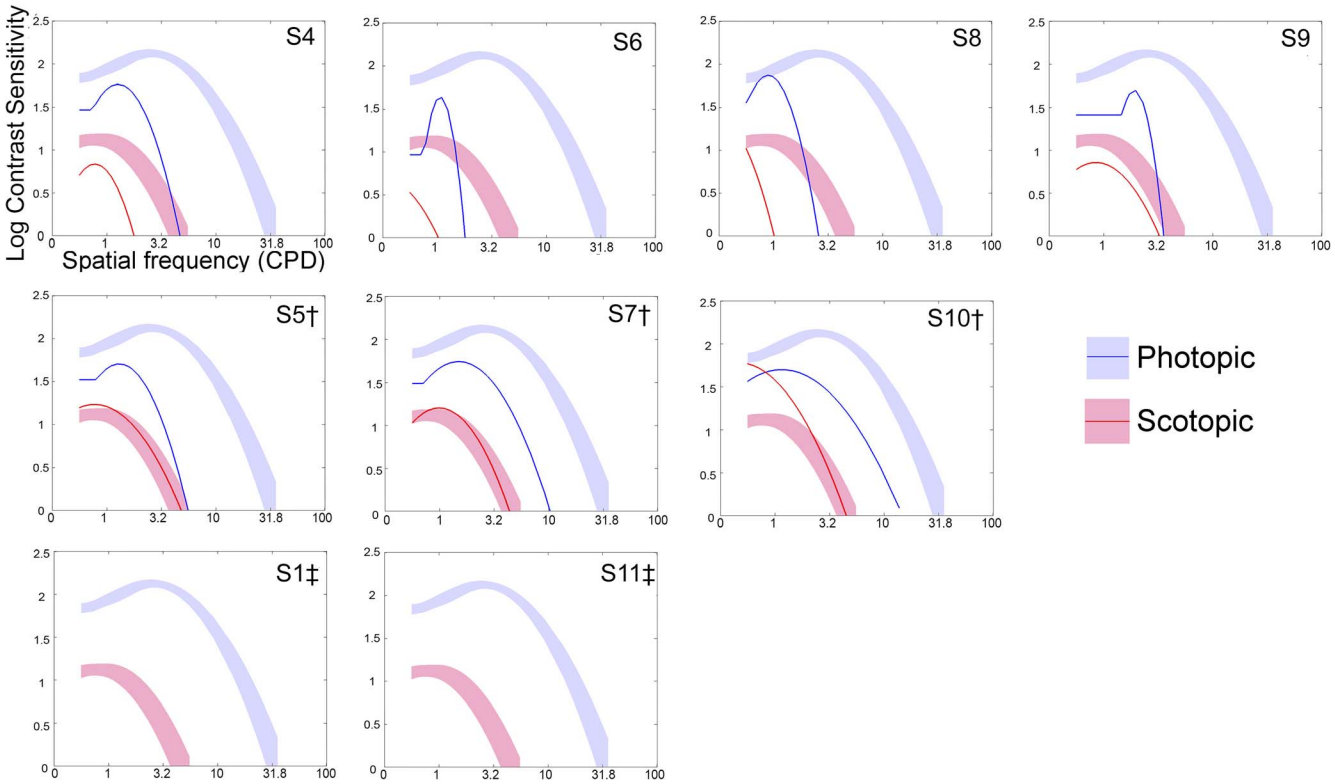

Figure 4. Contrast sensitivity functions (CSFs) for individual ACHM subjects. *Solid lines* represent CSFs for each light condition with *blue* representing photopic results and *red* representing scotopic results. *Shaded blue and red areas* represent the 95% confidence intervals of control data in the photopic and scotopic conditions, respectively. Subjects in the *top line* had CSF results below the control range. Subjects shown in the *middle line* had scotopic CSFs within the normal scotopic range and are marked †. Those with no recordable response are shown in the *bottom line* and marked ‡.

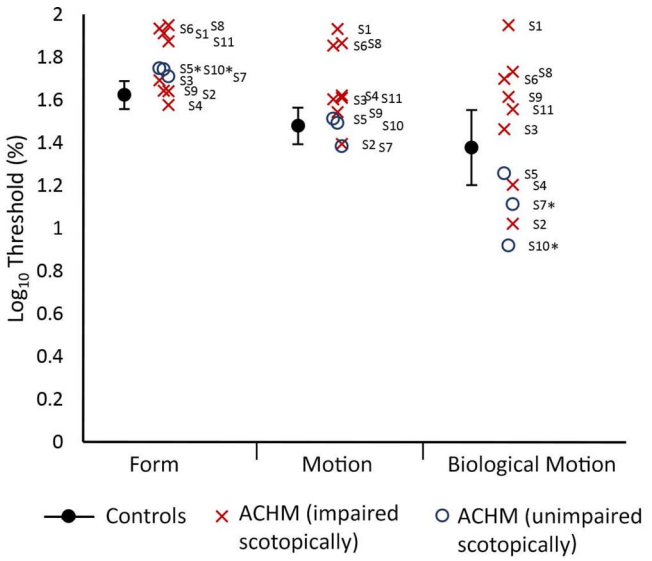

Figure 5. Form, motion, and biological motion thresholds in the scotopic condition. Control data represent the group mean; *error bars* represent the 95% confidence interval. Individual ACHM subjects (S5, S7, and S10) who had scotopic CSFs comparable to those of controls are plotted individually (O's) alongside the ACHM subjects with impaired scotopic CSFs (X's). Subjects S5 and S10 had significantly worse form thresholds than controls, while subjects S7 and S10 had significantly better biological motion thresholds than controls (differences significant after correction for multiple comparisons are marked *).

motion perception, but not others such as global form and motion perception. It may be that an absence of cones from birth allows for some specialization for scotopic vision.

Deficits relative to controls in scotopic conditions may be due to two main factors. First, they could be the outcome of atypical visual development. Second, results could be due to a loss of rod function relative to controls. A loss of rod sensitivity has been suggested in ACHM.[16–19,54,55] We gained insight into the extent to which there may have been such disruption from our measures of CSFs across different light levels.

Contrast sensitivity function results showed that most ACHM subjects had low-level deficits in spatial vision across both photopic and scotopic light conditions. These effects did not seem to be explained by either the age of subjects or their genotype, which varied across both the subgroup of subjects with normal scotopic CSF and those who showed minimal CSF responses.

In subjects with atypical scotopic CSF results, it is possible that there is rod dysfunction alongside cone dysfunction. Previous detailed reports of rod function in a single subject with ACHM described rod-mediated vision that was comparable to controls.[9–11] However, there is variation across individuals. Some cases of ACHM with associated rod dysfunction have been reported,[16,54,55] and atypical dark adaptation curves have been found.[17–19] Kahn et al.[54] reported on three sisters with cone disorders caused by the *CNGB3* genotype. Rod ERG revealed reduced b-wave amplitudes indicating loss of rod function. The results of our CSF test support the view that a majority of ACHM subjects had associated rod dysfunction, with six of nine ACHM subjects demonstrating reduced spatial vision at scotopic light levels. Possible reasons for rod dysfunction in ACHM subjects may be

the result of a bystander effect in which the loss of one class of photoreceptor contributes to the decline of other photoreceptors through the transfer of material through rod–cone gap junctions.[56]

Most strikingly, two of the three ACHM subjects with normal scotopic CSFs showed superior scotopic biological motion perception compared to controls with healthy vision. This implies that when low-level spatial vision is not impaired, some aspects of scotopic extrastriate vision in ACHM subjects can be better than in healthy controls. This would be explained by a developmental specialization for visual processing using only the rod signal. Whether this advantage for biological motion processing has any relationship to the observation by Sacks[57] that Pingelap islanders with ACHM are as good as or better than unaffected observers at seeing fish moving in the water at night is an interesting question for further research.

The dissociations in global form, motion, and biological motion processing, in which global form and motion are impaired but biological motion less so, are in line with evidence that the rod system may be optimized for some types of motion perception relative to form. Rods feed into magnocellular mechanisms within the visual cortex,[58–60] which in turn support dorsal stream processing and motion perception.[61] Parvocellular pathways, which support the perception of form via the ventral stream,[62–64] receive the majority of their input from cones,[59] and it is therefore understandable that cone disorder subjects would demonstrate impairments in form perception. Scotopic form impairments were still seen in two of three ACHM subjects with normal scotopic CSFs (suggesting normal low-level vision), which suggests atypical extrastriate processing due to development with atypical visual input. The cone signal therefore appears to play a crucial role in the development of perception of global form. In contrast, three of three ACHM subjects with normal scotopic CSFs showed global motion perception within the normal (control) range. This suggests that the global motion impairments seen in the main group of ACHM subjects could be explained by limitations in spatial vision due to impairments in rod functioning rather than by atypical development of extrastriate processing.

The sparing of biological motion perception in ACHM subjects follows similar findings in subjects with congenital cataracts and amblyopia.[28,65,66] These results all point toward biological motion perception being spared when vision is impaired. Achromatopsia, cataract, and amblyopia subjects reported in these studies have in common substantial visual impairment during early development. Visual development in these ACHM subjects may therefore have specialized to optimize detection of biological motion when visual information is sparse.

Cone dysfunction syndromes are a candidate for stem cell and gene therapy (Ye G, et al. *IOVS* 2014;55:ARVO E-Abstract 837).[4,67–69] The success of any new therapies will be dependent on the plasticity of both the retina and the visual brain to adapt to new visual input. The extent to which their midlevel visual processing can further be reorganized—for example, to improve the perception of global form given a newly available cone signal—is an important open question.

Acknowledgments

Supported by the Special Trustees of Moorfields Eye Hospital and the National Institute for Health Research (NIHR) Biomedical Research Centre at Moorfields Eye Hospital and the University College London (UCL) Institute of Ophthalmology. This work was funded by a UCL Grand Challenge Studentship.

Disclosure: **E. Burton**, None; **J. Wattam-Bell**, None; **G.S. Rubin**, None; **J. Aboshiha**, None; **M. Michaelides**, None; **J. Atkinson**, None; **O. Braddick**, None; **M. Nardini**, None

References

1. Aboshiha J, Dubis AM, Carroll J, Hardcastle AJ, Michaelides M. The cone dysfunction syndromes. *Br J Ophthalmol*. 2016;100:115–121.
2. Johnson S, Michaelides M, Aligianis IA, et al. Achromatopsia caused by novel mutations in both CNGA3 and CNGB3. *J Med Genet*. 2004;41:e20.
3. Remmer MH, Rastogi N, Ranka MP, Ceisler EJ. Achromatopsia: a review. *Curr Opin Ophthalmol*. 2015;26:333–340.
4. Komáromy AM, Alexander JJ, Rowlan JS, et al. Gene therapy rescues cone function in congenital achromatopsia. *Hum Mol Genet*. 2010;19:2581–2593.
5. Aboshiha J, Dubis AM, Cowing J, et al. A prospective longitudinal study of retinal structure and function in achromatopsia. *Invest Ophthalmol Vis Sci*. 2014;55:5733–5743.
6. Thiadens AAHJ, Somervuo V, van den Born LI, et al. Progressive loss of cones in achromatopsia: an imaging study using spectral-domain optical coherence tomography. *Invest Ophthalmol Vis Sci*. 2010;51:5952–5957.
7. Thomas MG, McLean RJ, Kohl S, Sheth V, Gottlob I. Early signs of longitudinal progressive cone photoreceptor degeneration in achromatopsia. *Br J Ophthalmol*. 2012;96:1232–1236.
8. Eksandh L, Kohl S, Wissinger B. Clinical features of achromatopsia in Swedish patients with defined genotypes. *Ophthalmic Genet*. 2002;23:109–120.
9. Hess RF, Nordby K, Pointer JS. Regional variation of contrast sensitivity across the retina of the achromat: sensitivity of human rod vision. *J Physiol*. 1987;388:101–119.
10. Hess RF, Nordby K. Spatial and temporal limits of vision in the achromat. *J Physiol*. 1986;371:365–385.
11. Hess RF, Nordby K. Spatial and temporal properties of human rod vision in the achromat. *J Physiol*. 1986;371:387–406.
12. Michaelides M, Holder GE, Hunt DM, Fitzke FW, Bird AC, Moore AT. A detailed study of the phenotype of an autosomal dominant cone-rod dystrophy (CORD7) associated with mutation in the gene for RIM1. *Br J Ophthalmol*. 2005;89:198–206.
13. Michaelides M. Cone and cone–rod dystrophies. In: *Inherited Chorioretinal Dystrophies*. Berlin, Heidelberg: Springer; 2014:151–163.
14. Sloan LL, Feiock K. Acuity-luminance function in achromatopsia and in progressive cone degeneration: factors related to individual differences in tolerance to bright light. *Invest Ophthalmol Vis Sci*. 1972;11:862–868.
15. Sloan LL. Congenital achromatopsia: a report of 19 cases. *J Opt Soc Am*. 1954;44:117–128.
16. Nishiguchi KM, Sandberg MA, Gorji N, Berson EL, Dryja TP. Cone cGMP-gated channel mutations and clinical findings in patients with achromatopsia, macular degeneration, and other hereditary cone diseases. *Hum Mutat*. 2005;25:248–258.
17. Aboshiha J, Luong V, Cowing J, et al. Dark-adaptation functions in molecularly confirmed achromatopsia and the implications for assessment in retinal therapy trials. *Invest Ophthalmol Vis Sci*. 2014;55:6340–6349.
18. Frey RG, Gordesch J, Heilig P, Thaler A. Dark adaptation in achromats (mathematical analysis) (author's translation) [in German]. *Albrecht Von Graefes Arch Klin Exp Ophthalmol*. 1975;196:299–302.
19. Simunovic MP, Regan BC, Mollon JD. Is color vision deficiency an advantage under scotopic conditions? *Invest Ophthalmol Vis Sci*. 2001;42:3357–3364.
20. Atkinson J, Wattam-Bell J, Braddick O, Birtles D, Barnett A, Cowie D. Form vs motion coherence sensitivity in infants: the dorsal/ventral developmental debate continues. *J Vis*. 2004;4(8):32.

21. Braddick O, Atkinson J, Wattam-Bell J. Normal and anomalous development of visual motion processing: motion coherence and "dorsal-stream vulnerability." *Neuropsychologia*. 2003;41:1769–1784.
22. Golarai G, Liberman A, Yoon JM, Grill-Spector K. Differential development of the ventral visual cortex extends through adolescence. *Front Hum Neurosci*. 2010;3:1–19.
23. Gunn A, Cory E, Atkinson J, et al. Dorsal and ventral stream sensitivity in normal development and hemiplegia. *Neuroreport*. 2002;13:843–847.
24. Atkinson J, King J, Braddick O, Nokes L, Anker S, Braddick F. A specific deficit of dorsal stream function in Williams' syndrome. *Neuroreport*. 1997;8:1919–1922.
25. Ellemberg D, Lewis TL, Maurer D, Brar S, Brent HP. Better perception of global motion after monocular than after binocular deprivation. *Vision Res*. 2002;42:169–180.
26. Kogan CS, Bertone A, Cornish K, et al. Integrative cortical dysfunction and pervasive motion perception deficit in fragile X syndrome. *Neurology*. 2004;63:1634–1639.
27. Lewis TL, Ellemberg D, Maurer D, et al. Sensitivity to global form in glass patterns after early visual deprivation in humans. *Vision Res*. 2002;42:939–948.
28. Neri P, Luu JY, Levi DM. Sensitivity to biological motion drops by 1/2 log-unit with inversion, and is unaffected by amblyopia. *Vision Res*. 2007;47:1209–1214.
29. Taylor NM, Jakobson LS, Maurer D, Lewis TL. Differential vulnerability of global motion, global form, and biological motion processing in full-term and preterm children. *Neuropsychologia*. 2009;47:2766–2778.
30. Braddick OJ, O'Brien JM, Wattam-Bell J, Atkinson J, Hartley T, Turner R. Brain areas sensitive to coherent visual motion. *Perception*. 2001;30:61–72.
31. Burnat K, Stiers P, Arckens L, Vandenbussche E, Zernicki B. Global form perception in cats early deprived of pattern vision. *Neuroreport*. 2005;16:751–754.
32. El-Shamayleh Y, Kiorpes L, Kohn A, Movshon JA. Visual motion processing by neurons in area MT of macaque monkeys with experimental amblyopia. *J Neurosci*. 2010;30:12198–12209.
33. Gallant JL, Shoup RE, Mazer JAA. Human extrastriate area functionally homologous to macaque V4. *Neuron*. 2000;27:227–235.
34. Grossman ED, Blake R. Brain areas active during visual perception of biological motion. *Neuron*. 2002;35:1167–1175.
35. Kiorpes L, Price T, Hall-Haro C, Movshon JA. Development of sensitivity to global form and motion in macaque monkeys (*Macaca nemestrina*). *Vision Res*. 2012;63:34–42.
36. Zapasnik M, Burnat K. Binocular pattern deprivation with delayed onset has impact on motion perception in adulthood. *Neuroscience*. 2013;255:99–109.
37. Burton EA, Wattam-Bell J, Rubin GS, Atkinson J, Braddick O, Nardini M. The effect of blur on cortical responses to global form and motion. *J Vis*. 2015;15(15):12.
38. Burton E, Wattam-Bell J, Rubin GS, Atkinson J, Braddick O, Nardini M. Cortical processing of global form, motion and biological motion under low light levels. *Vision Res*. 2016;121:39–49.
39. Essock EA, Williams RA, Enoch JM, Raphael S. The effects of image degradation by cataract on vernier acuity. *Invest Ophthalmol Vis Sci*. 1984;25:1043–1050.
40. Williams RA, Enoch JM, Essock EA. The resistance of selected hyperacuity configurations to retinal image degradation. *Invest Ophthalmol Vis Sci*. 1984;25:389–399.
41. Legge GE, Pelli DG, Rubin GS, Schleske MM. Psychophysics of reading—I. Normal vision. *Vision Res*. 1985;25:239–252.
42. Billino J, Bremmer F, Gegenfurtner KR. Motion processing at low light levels: differential effects on the perception of specific motion types. *J Vis*. 2008;8(3):14.
43. Grossman ED, Blake R. Perception of coherent motion, biological motion and form-from-motion under dim-light conditions. *Vision Res*. 1999;39:3721–3727.
44. Gegenfurtner KR, Mayser HM, Sharpe LT. Motion perception at scotopic light levels. *J Opt Soc Am A Opt Image Sci Vis*. 2000;17:1505–1515.
45. Chaparro A, Young RS. Reading with rods: the superiority of central vision for rapid reading. *Invest Ophthalmol Vis Sci*. 1993;34:2341–2347.
46. Brainard DH. The Psychophysics Toolbox. *Spat Vis*. 1997;10:433–436.
47. Kleiner M, Brainard D, Pelli D, Ingling A, Murray R, Broussard C. What's new in Psychtoolbox-3. *Perception*. 2007;36:1.
48. Pelli DG. The VideoToolbox software for visual psychophysics: transforming numbers into movies. *Spat Vis*. 1997;10:437–442.
49. Atkinson J, Braddick O. Dorsal stream vulnerability and autistic disorders: the importance of comparative studies of form and motion coherence in typically developing children and children with developmental disorders. *Curr Psychol Cogn*. 2005;23:49–58.
50. Wattam-Bell J, Birtles D, Nyström P, et al. Reorganization of global form and motion processing during human visual development. *Curr Biol*. 2010;20:411–415.
51. Kontsevich LL, Tyler CW. Bayesian adaptive estimation of psychometric slope and threshold. *Vision Res*. 1999;39:2729–2737.
52. Cutting JE. A program to generate synthetic walkers as dynamic point-light displays. *Behav Res Methods*. 1978;10:91–94.
53. Lesmes LA, Lu Z-L, Baek J, Albright TD. Bayesian adaptive estimation of the contrast sensitivity function: the quick CSF method. *J Vis*. 2010;10(3):17.
54. Khan NW, Wissinger B, Kohl S, Sieving PA. *CNGB3* achromatopsia with progressive loss of residual cone function and impaired rod-mediated function. *Invest Ophthalmol Vis Sci*. 2007;48:3864–3871.
55. Sundin OH, Yang JM, Li Y, et al. Genetic basis of total colourblindness among the Pingelapese islanders. *Nat Genet*. 2000;25:289–293.
56. Besharse J, Bok D. *The Retina and Its Disorders*. Cambridge, MA: Academic Press; 2011:930.
57. Sacks O. *The Island of the Colour-Blind*. London, UK: Pan Macmillan; 1996.
58. Chen J, Sampath AP. Structure and function of rod and cone photoreceptors. In: Ryan SJ, Schachat AP, Wilkinson CP, et al., eds. *Retina*. 5th ed. London: W.B. Saunders; 2013:342–359.
59. Lee BB, Smith VC, Pokorny J, Kremers J. Rod inputs to macaque ganglion cells. *Vision Res*. 1997;37:2813–2828.
60. Sun H, Pokorny J, Smith VC. Rod-cone interactions assessed in inferred magnocellular and parvocellular postreceptoral pathways. *J Vis*. 2001;1(1):5.
61. Maunsell JH, Nealey TA, DePriest DD. Magnocellular and parvocellular contributions to responses in the middle temporal visual area (MT) of the macaque monkey. *J Neurosci*. 1990;10:3323–3334.
62. Wilkinson F, James TW, Wilson HR, Gati JS, Menon RS, Goodale MA. An fMRI study of the selective activation of human extrastriate form vision areas by radial and concentric gratings. *Curr Biol*. 2000;10:1455–1458.
63. Wilson HR, Wilkinson F, Asaad W. Concentric orientation summation in human form vision. *Vision Res*. 1997;37:2325–2330.
64. Wilson HR, Wilkinson F. Detection of global structure in Glass patterns: implications for form vision. *Vision Res*. 1998;38:2933–2947.

Investigative Ophthalmology & Visual Science

65. Hadad BS, Maurer D, Lewis TL. Sparing of sensitivity to biological motion but not of global motion after early visual deprivation. *Dev Sci*. 2012;15:474–481.
66. Thompson B, Troje NF, Hansen BC, Hess RF. Amblyopic perception of biological motion. *J Vis*. 2008;8(4):22.
67. Banin E, Gootwine E, Obolensky A, et al. Gene augmentation therapy restores retinal function and visual behavior in a sheep model of CNGA3 achromatopsia. *Mol Ther*. 2015;23:1423–1433.
68. Sundaram V, Wilde C, Aboshiha J, et al. Retinal structure and function in achromatopsia: implications for gene therapy. *Ophthalmology*. 2014;121:234–245.
69. Yang P, Michaels KV, Courtney RJ, et al. Retinal morphology of patients with achromatopsia during early childhood: implications for gene therapy. *JAMA Ophthalmol*. 2014;132:823–831.

Investigative Ophthalmology & Visual Science